Hindawi
Advances in Civil Engineering
Volume 2024, Article ID 1137438, 14 pages
https://doi.org/10.1155/2024/1137438

*Research Article*

# Research on Flexural Properties and Flexural Toughness Evaluation Method of Steel Fiber Reinforced Cementitious Composites under Polar Low Temperatures

**Farun Shui**,[1] **Jun Su**,[1,2] **Junjie Huang**,[1] **Yang Li**,[1] **and Weimin Qian**[1]

[1]*School of Civil Engineering Architecture and Environment, Hubei University of Technology, Wuhan 430068, China*
[2]*Key Laboratory of Intelligent Health Perception and Ecological Restoration of Rivers and Lakes, Ministry of Education, Hubei University of Technology, Wuhan 430068, China*

Correspondence should be addressed to Jun Su; 19981037@hbut.edu.cn

Received 7 March 2023; Revised 25 October 2023; Accepted 15 February 2024; Published 29 February 2024

Academic Editor: Dario De Domenico



In this research, five groups of steel fiber reinforced cementitious composite (SFRCC) with different fiber volume content (0%, 0.5%, 1.0% 1.5%, and 2.0%) were designed to perform four-point flexural tests on beam specimens to study the effects of polar temperature (20, 0, −25, −50, −75, and −100°C) and fiber volume content on the flexural properties. The flexural toughness index and load holding capacity index were calculated based on the load–displacement curve, and the enhancement and toughening mechanisms of SFRCC by low temperature and steel fibers were analyzed in conjunction with experimental observations. The results of the proposed flexural toughness evaluation method show that the flexural toughness of SFRCC can significantly improve than that of ambient temperature when the temperature is lower than 0°C. With the decrease in temperature, the flexural property of SFRCC increases first and then decreases, and the temperature point of this transition is around −50–−75°C. The flexural property enhancement effect of 1.0% fiber volume content SFRCC is more significant in low temperatures according to the flexural toughness index and load holding capacity index. The conclusion can provide a reference for the application of SFRCC in cryogenic engineering, as well as a simple and quantifier evaluation method for flexural toughness is proposed.

## 1. Introduction

The polar region is rich in oil, gas, and mineral resources, making them crucial areas for human development and addressing energy shortages. According to the assessment report of the United States Geological Survey (USGS) in 2008, there are $143 \times 10^8\,m^3$ of recoverable oil reserves and $47 \times 10^{12}\,m^3$ of natural gas reserves waiting to be discovered in the Arctic region, accounting for about 13% of the world's undiscovered oil reserves and 30% of the world's unexploited natural gas reserves [1]. Hence, the development and utilization of polar energy make it necessary to construct civil engineering projects in polar regions.

However, the polar region is in an extremely cold environment all the year-round. According to relevant literature reports, the lowest temperature in the Antarctic can reach −89°C, and the lowest temperature in the Arctic can reach −69°C [2], there is also permafrost [3], which significantly reduces the performance of concrete and shortens the service life of engineering structures [4], which poses new requirements for the performance of concrete materials widely used in the field of civil engineering. Existing research results show that the strength of cement mortar subjected to low temperature is affected by water–cement ratio, curing time, porosity freezing degree, and water content [5], and low-temperature action and water content have obvious effects on the compressive and tensile strength of concrete while the strength grade has relatively small effects [6, 7]. However, current research on the mechanical properties of concrete materials subjected to low-temperature conditions primarily focuses on compressive and tensile performance, while there is relatively less research on flexural performance.

Steel fiber reinforced cementitious composite (SFRCC) has excellent mechanical properties and deformation properties

Table 1: Physical parameters of steel fiber.

| Density (g·cm$^{-3}$) | Diameter (mm) | Length (mm) | Tensile strength (MPa) | Elastic modulus (GPa) |
|---|---|---|---|---|
| 7.8 | 0.2 | 13 | ≥2,000 | 200 |

Table 2: Number and mix proportion of specimens.

| Specimen number | Fiber content (vol%) | Cement (kg·m$^{-3}$) | Sand (kg·m$^{-3}$) | Water (kg·m$^{-3}$) | Fly ash (kg·m$^{-3}$) |
|---|---|---|---|---|---|
| 0vol% | 0 | | | | |
| 0.5vol% | 0.5 | | | | |
| 1.0vol% | 1.0 | 680 | 1,200 | 247 | 170 |
| 1.5vol% | 1.5 | | | | |
| 2.0vol% | 2.0 | | | | |

[8], in ambient temperature, steel fiber can improve the flexural tensile strength and flexural toughness of the matrix obviously, as well as it is an excellent material for improving the seismic performance and durability of engineering structures [9, 10]. Rostásy and Sprenger [11] studied the compressive and tensile properties of steel fiber reinforced concrete (SFRC), and the results showed that adding steel fiber could significantly reduce the concrete damage caused by temperature decrease. Kim et al. [12] studied the compressive and tensile properties of ultrahigh performance fiber reinforced concrete (UHPFRC) doped with straight bar steel fiber under ultralow temperature (−170°C), and the results showed that the compressive and tensile properties of UHPFRC were significantly improved compared with that at ambient temperature. Pigeon and Cantin [13] conducted a study on the flexural properties of SFRC, showing that temperature reduction can enhance the flexural toughness of SFRC within the range of 20–−30°C, however, the study on flexural properties at a lower temperature is limited. Therefore, studying the flexural performance of SFRCC at even lower temperatures is of great significance.

This study aims to investigate the flexural performance of SFRCC in the temperature range of 0–−100°C based on four-point flexural tests to meet the requirements of concrete materials for engineering construction in polar regions. By analyzing the failure modes and flexural performance indicators of SFRCC under low-temperature conditions, the mechanisms of strengthening and toughening due to low temperature and steel fibers are revealed. In addition, the proposed method for evaluating the flexural toughness of SFRCC under low temperatures can serve as a reference for the construction of low-temperature engineering.

## 2. Experimental Program

*2.1. Mixture Proportions.* The specimen size was 100 mm × 100 mm × 400 mm. P.O.42.5 ordinary Portland cement of Huaxin brand and GradeIfly ash from the Wuhan Yangluo power plant were used. Natural river sand with fineness modulus 2.3 and melamine F10 polycarboxylic acid highly efficient water-reducing agent was used for the specimen. The steel fiber adopts straight rod-shaped copper-plated microwire steel fiber, and its physical parameters are shown in Table 1. In the flexural test, the fiber volume content of SFRCC was 0%, 1.0%, 1.5%, and 2.0%, and the temperature points of the specimens subjected were 20, 0, −25, −50, −75, and −100°C, respectively. The number and mix ratio of specimens are shown in Table 2. Three cubes with sides length of 100 mm were made of SFRCC containing each fiber volume, and a 28 days compressive strength test was carried out according to GB/T [14] 50081-2019. The average compressive strength of SFRCC cubes is shown in Table 3, and the specimen preparation process of SFRCC is shown in Figure 1.

Table 3: Cube compressive strength of SFRCC.

| Fiber content (vol%) | 0 | 0.5 | 1.0 | 1.5 | 2.0 |
|---|---|---|---|---|---|
| Mean compressive strength (MPa) | 32.3 | 35.4 | 39.8 | 41.9 | 44.4 |

*2.2. Experimental Setups and Process.* The self-made cryogenic test chamber is used for cooling equipment, as shown in Figure 2(a). Liquid nitrogen is injected into the cooling chamber, and the cooling rate is controlled at 1.5°C/min. The Pt100 thermocouple is embedded in the specimen to detect the core temperature of the specimen during the cooling process. When the target temperature is reached, the specimen is taken out and placed in an incubator made of polyurethane material, and then the next test is carried out. The control method of temperature accuracy in the test is consistent with Xie et al. [15].

According to CECS 13:2009 [16] and GB/T 50152-2012 [17], an MTS CBT1105-D microcomputer-controlled flexural testing machine was used to carry out the flexural test. The schematic diagram is shown in Figure 2(b).

Generally, in the elastic stage before SFRCC reaches the peak load, the loading mode controlled by the load can be used. After the peak load is exceeded, the SFRCC will soften during the loading process, so the displacement-controlled loading mode should be adopted after the peak load. However, when the loading mode is changed from load-controlled to displacement-controlled, the flexural load–displacement curve will not be smooth at the elastic limit position of SFRCC. To obtain a stable load–displacement curve, a four-point flexural test was carried out on five groups of SFRCC specimens using a displacement-controlled loading method to study the influence of low temperature and fiber volume

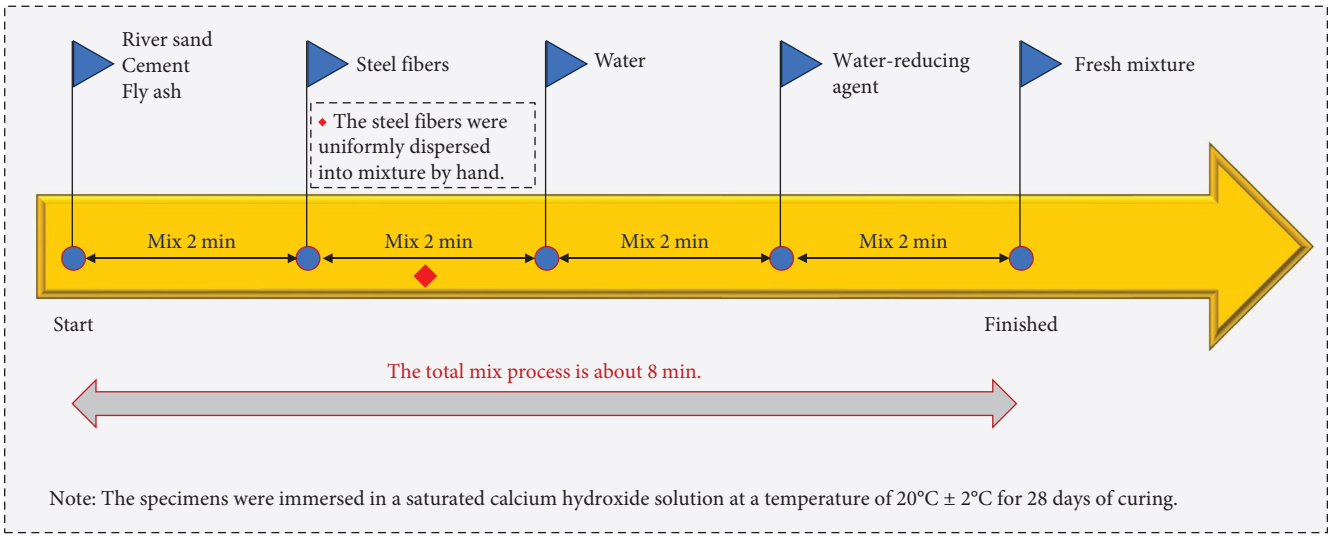


Figure 1: Specimen preparation process of SFRCC.

content on the flexural properties of SFRCC. The loading rate was 0.5 mm/min, the maximum test force of the measuring instrument was 100 kN, and the force control speed adjustment range of the measuring instrument was 0.02%–5% FS/s.

## 3. Experimental Results

The load–displacement curve of specimens with different fiber content under loading is shown in Figure 3. The test process can be divided into three stages: the precracking stage, the crack development stage, and the failure stage. Figure 3(a) shows the load–displacement curve of the cement base matrix without steel fiber. It can be seen that: in the flexural process, with the increase of load, vertical cracks developing along the section suddenly appear in the middle of the specimen and rapidly run through the whole section, and fracture occurs along with violent sound, showing the brittle failure characteristic of "cracking is fracture." The flexural strength of the SFRCC matrix increases with the decrease in temperature, which is similar to the conclusion of Browne and Bamfourth [18]. The maximum improvement of bearing capacity of the SFRCC matrix is about 355% at −100°C.

The load–displacement curves of the 0.5vol% specimen are shown in Figure 3(b). Before cracking, the load of the specimen is small, and the load and displacement of the specimen are small too, at this time SFRCC is in the elastic stage. As the load gradually increases and the matrix reaches the maximum tensile strain, small cracks appear at the bottom of the specimen, and stress concentration occurs at the crack tip and begins to develop vertically along the section. In this case, steel fiber plays a bridging role at the crack, alleviating the surge of stress at the crack tip and evenly transferring it to the uncracked matrix near the fiber. The bridging effect of steel fiber restricts the further development of cracks. The brittle failure characteristics disappear and ductility increases. When the load increased to about 90% of the peak load, the section crack developed into a main crack and extended to the top of the specimen. The width of the crack and the deflection of the specimen increased significantly, but no brittle failure characteristics appeared. Finally, the failure was caused by the collapse of the matrix at the top of the specimen and the support. The test phenomena of SFRCC specimens of 1.0vol%, 1.5vol%, and 2.0vol % are the same as those of 0.5vol%, showing the characteristics of "cracking but no fracture", because of that, when the displacement exceeds 1/75 of the span, the specimens are considered to have failed and stopped working. SFRCC specimens subjected to low temperature did not show matrix spalling, outer bulge, as well as missing edges and corners, and the whole specimen maintained good integrity. The failure diagram of the specimen is shown in Figure 4.

Figure 5 shows the typical load–displacement curve of the steel fiber pullout test. Combined with Figure 3, it can be seen that: when the temperature is relatively high, the load–displacement curve of SFRCC shows the phenomenon of slip hardening in which the bearing capacity first decreases and then increases. The reason is that parts of the matrix adhere to the fiber surface and slide along with the fiber in the process of pulling out the steel fiber after unbinding with the matrix, which leads to the blockage of the slip channel and the increase of sliding friction force. However, with the decrease in temperature, the slip-hardening phenomenon disappears and the slip-softening phenomenon occurs because low temperature not only enhances the bonding property of steel fiber and matrix but also increases the bonding strength of the SFRCC matrix itself. After the steel fiber is unglued, the matrix is no longer attached to the fiber surface [12], and the slip channel is no longer blocked. The load–displacement curve presents a slip-softening phenomenon, but the ultimate load increases greatly due to the increase of energy required to pull out the steel fiber.

The peak displacement and peak load of SFRCC at different temperatures are shown in Figure 6. Compared with 0.5vol%, 1.0vol%, 1.5vol%, and 2.0vol%, the average increase of peak load of SFRCC respectively 85.64%, 96.22%, and 125.86%. The average increase of peak displacement is respectively 30.46%, 21.00%, and 30.87%, indicating that fiber content


(a)

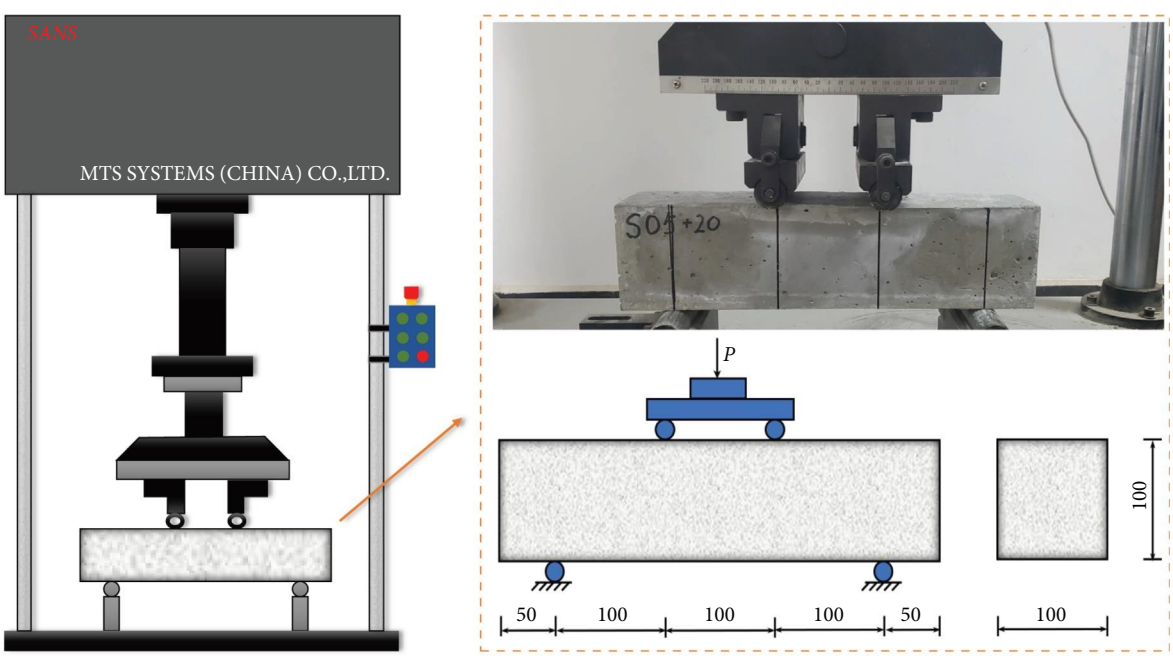


(b)

Figure 2: Test equipment: (a) cooling setup and (b) loading diagram.

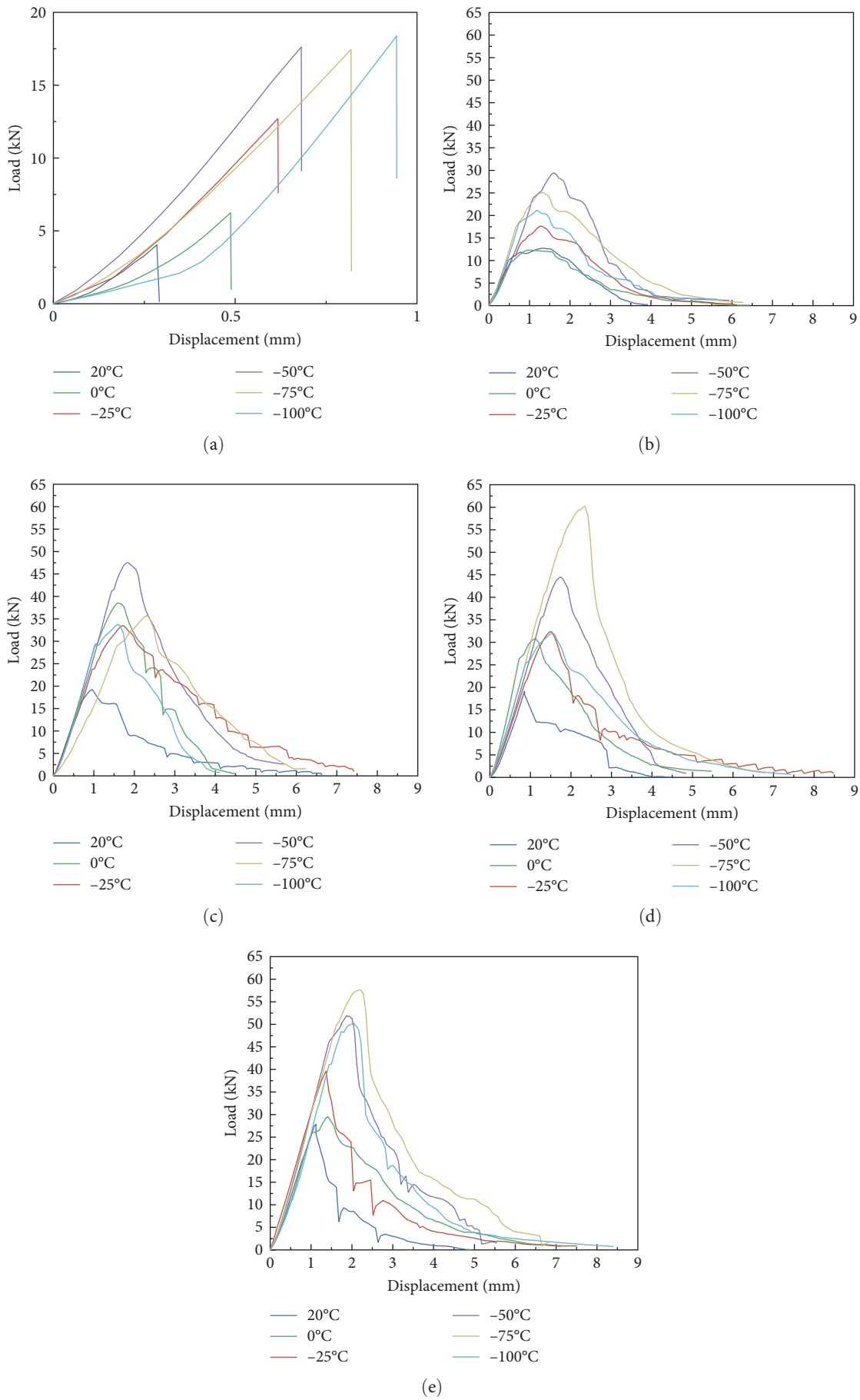


Figure 3: Flexural load–displacement curves of SFRCC at different temperatures: (a) 0vol%, (b) 0.5vol%, (c) 1.0vol%, (d) 1.5vol%, and (e) 2.0vol%.

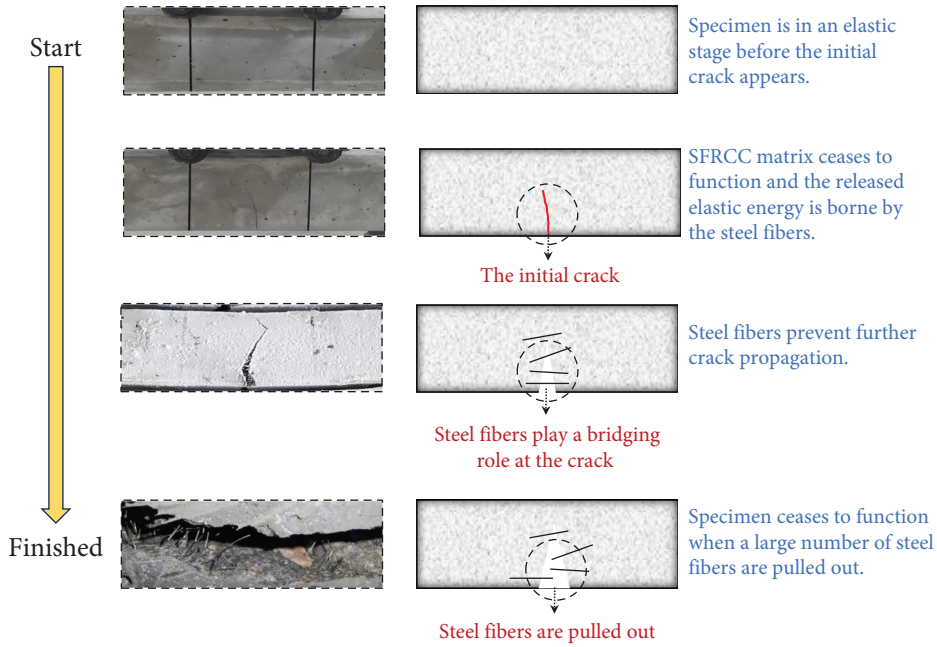


Figure 4: Failure mode of SFRCC.

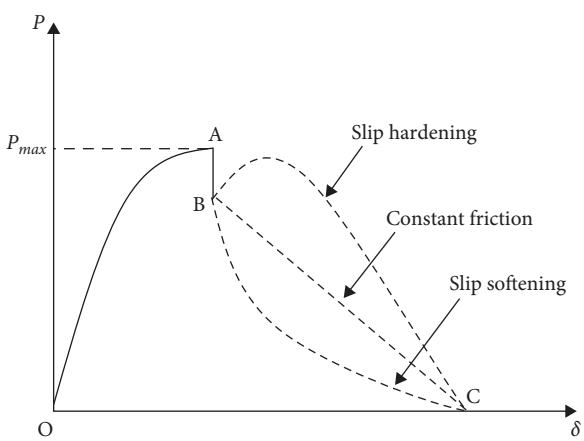


Figure 5: Typical load–displacement curve of steel fiber pullout test.

can significantly affect the peak load and deformation capacity of SFRCC, but has little effect on the peak displacement.

The compressive strength and flexural strength of SFRCC in ambient temperature are shown in Figure 7. From Figure 7(a), it can be observed that with an increase in fiber volume fraction, both the compressive strength and flexural strength exhibit a similar linear increasing trend. This indicates that the addition of steel fibers in the SFRCC matrix effectively enhances its compressive and flexural performance. From Figure 7(b), it can be seen that there is a linear correlation between the compressive strength and flexural strength of SFRCC. Improving the compressive strength of SFRCC also leads to an improvement in its flexural strength, suggesting that the flexural performance can be enhanced by increasing the strength grade of the SFRCC matrix. Additionally, studies by Shi et al. [19] have found that in low-temperature environments, there is a significant difference in the increment of compressive strength among different strength grades of concrete, deviating from a linear trend. The higher the strength grade, the greater the absolute increment in compressive strength, while the relative increment becomes smaller.

## 4. Evaluation of SFRCC Flexural Toughness

*4.1. Evaluation Method of Matrix Flexural Toughness.* Toughness is a reflection of the deformation work absorbed per unit volume when the material deforms under the action of external forces until failure. Since the matrix of SFRCC is a brittle failure, according to the definition of toughness, the flexural toughness of the SFRCC matrix can be characterized by the amount of energy absorbed in the deformation process. The calculation expression is shown in Equation (1).

$$W = \int P \mathrm{d}\delta. \tag{1}$$

*4.2. Evaluation Method of SFRCC Flexural Toughness at Ambient Temperature.* Currently, the flexural toughness of fiber-reinforced concrete is mainly evaluated from the perspectives of equivalent flexural strength and energy absorption. There are commonly used JSCE-SF4 [20] standards for evaluating flexural properties based on equivalent flexural strength and ASTM C 1609 [21] standards for evaluating energy absorption capacity. However, the flexural toughness of SFRCC used to evaluate the effect of low temperature is slightly inadequate.

The evaluation method of flexural toughness is shown in Figure 8. JSCE-SF4 [20] standard used equivalent flexural strength to evaluate the flexural toughness of concrete, and its calculation formula is as follows:

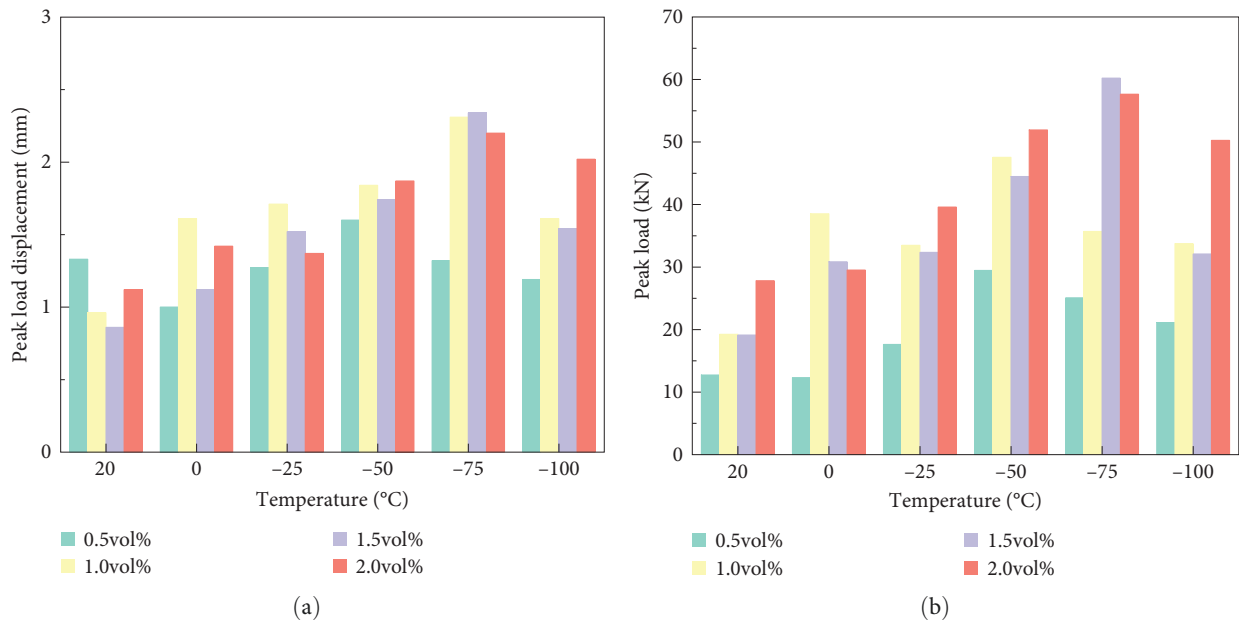


Figure 6: Displacement at the peak load and peak load of SFRCC at different temperatures: (a) peak load displacement and (b) peak load.

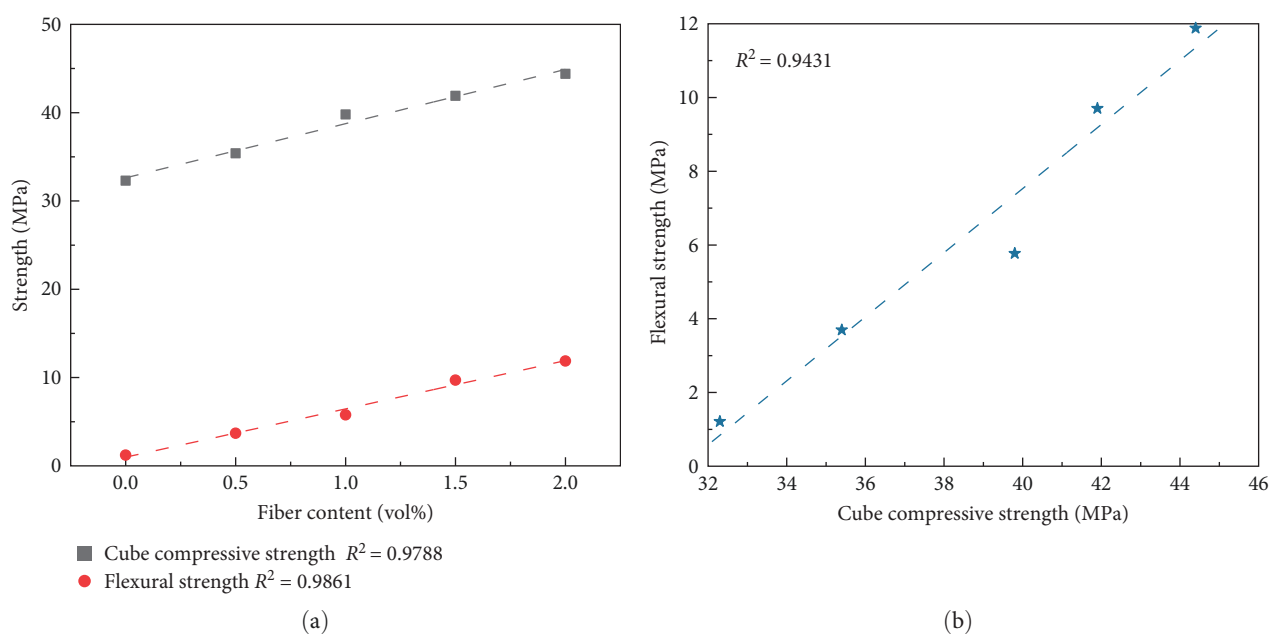


Figure 7: Flexural strength and cube compressive strength of SFRCC at ambient temperature: (a) the relationship between fiber content and strength and (b) the relationship between flexural strength and compressive strength.

$$\sigma_b = \frac{T_b}{\delta_{tb}} \cdot \frac{L}{bh^2}, \tag{2}$$

where $\sigma_b$ (MPa) is equivalent flexural strength; $\delta_{tb}$ (mm) is the displacement with a calculated displacement of L/150; and $T_b$ (N·mm) is the area enclosed by SFRCC load–displacement curve from the origin to L/150, which is the area enclosed by OEG curve in Figure 8. $L$ (mm) is the span between the test beam supports; $b$ (mm) is the section width; and $h$ (mm) is the height of the section.

JSCE-SF4 [20] standard has the advantages of a clear concept, simple calculation, and not being affected by the position of the initial crack point. The toughness results of SFRCC calculated according to Equation (2) are shown in Table 4. As can be seen: for SFRCC subjected to low temperature, low temperature will enhance the flexural toughness of the matrix [13], while steel fibers are inactive before the matrix cracking [22], which leads the part of the toughness enhancement of the matrix by low temperature in the rising stage will be calculated into the toughening effect of steel fibers when evaluating the toughness

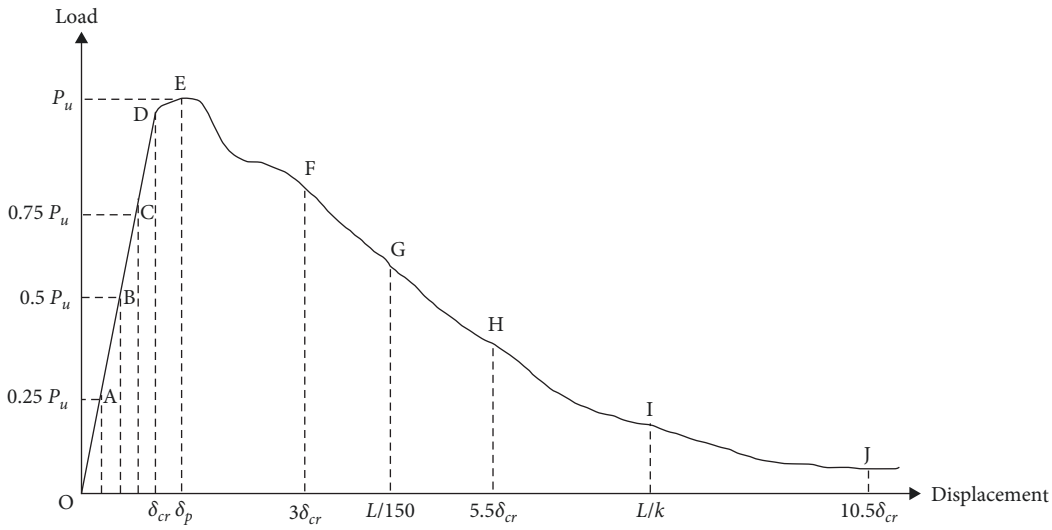


Figure 8: Definition of flexural toughness indexes.

Table 4: Calculation results of $\sigma_b$.

| Specimen number | Temperature (°C) | $\sigma_b$ (MPa) | Specimen number | Temperature (°C) | $\sigma_b$ (MPa) |
|---|---|---|---|---|---|
| 0.5vol% | 20 | 2.97 | 1.0vol% | 20 | 3.83 |
| | 0 | 2.82 | | 0 | 7.14 |
| | −25 | 3.69 | | −25 | 6.29 |
| | −50 | 5.42 | | −50 | 7.86 |
| | −75 | 5.19 | | −75 | 4.93 |
| | −100 | 4.48 | | −100 | 6.39 |
| 1.5vol% | 20 | 3.18 | 2.0vol% | 20 | 4.14 |
| | 0 | 6.17 | | 0 | 5.61 |
| | −25 | 5.90 | | −25 | 6.88 |
| | −50 | 7.60 | | −50 | 8.75 |
| | −75 | 8.72 | | −75 | 8.77 |
| | −100 | 6.36 | | −100 | 7.76 |

of low-temperature SFRCC. As a result, the calculation results are too large, which cannot fully reflect the toughening effect of steel fiber on the matrix. Moreover, the peak displacement of SFRCC increased due to low temperature, which made the peak displacement exceed the calculated displacement $L/150$ (such as 1.5vol%), which could not reflect the enhancement effect of steel fiber on postpeak toughness.

ASTM C 1609 [21] standard used the flexural toughness index $I_5$, $I_{10}$, and $I_{20}$ to evaluate the flexural toughness of concrete. The calculation formula is as follows:

$$\begin{cases} I_5 = \dfrac{\Omega_{3\delta_{cr}}}{\Omega_{\delta_{cr}}} \\ I_{10} = \dfrac{\Omega_{5.5\delta_{cr}}}{\Omega_{\delta_{cr}}} \\ I_{20} = \dfrac{\Omega_{10.5\delta_{cr}}}{\Omega_{\delta_{cr}}} \end{cases}, \tag{3}$$

where $\delta_{cr}$ (mm) is the displacement corresponding to the initial crack point; $\Omega_{\delta cr}$, $\Omega_{3\delta cr}$, $\Omega_{5.5\delta cr}$, and $\Omega_{10.5\delta cr}$ (N·mm) is the area under the load–displacement curve when the displacement is calculated as $\delta_{cr}$, $3\delta_{cr}$, $5.5\delta_{cr}$, and $10.5\delta_{cr}$, namely the area surrounded by OD, OEF, OEH, and OEI curves in Figure 8.

The physical significance of this method is clear and it is not affected by specimen size. However, since steel fibers have little influence on the cracking point and the low temperature will strengthen the matrix strength and bring the initial cracking point closer to the peak point, the $5.5\delta_{cr}$ and $10.5\delta_{cr}$ points in the load–displacement curve of SFRCC appear after the failure displacement, as well as the flexural toughness properties of SFRCC cannot be fully evaluated.

*4.3. Evaluation Method of SFRCC Flexural Toughness at Low Temperature.* Combined with the characteristics of SFRCC material, the toughening effect of steel fiber on the matrix before peak load is mainly manifested in the enhancement of peak displacement, peak strength, and toughness after cracking, and the toughening effect on the matrix after peak load is mainly manifested in the enhancement of residual toughness and load holding properties. Based on the evaluation method of

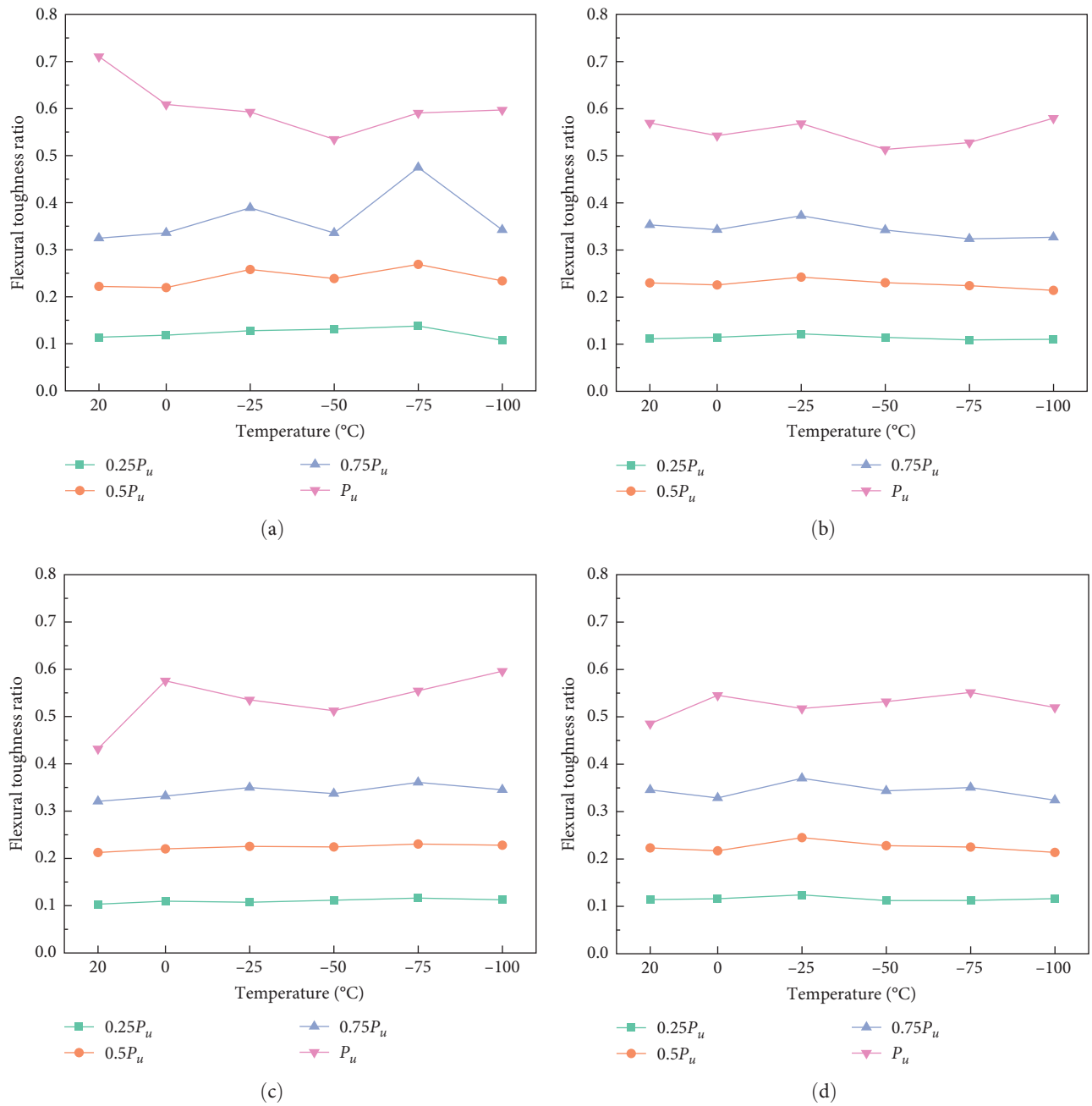


Figure 9: Flexural toughness ratio of SFRCC under prepeak load: (a) 0.5vol%, (b) 1.0vol%, (c) 1.5vol%, and (d) 2.0vol%.

flexural toughness of SFRCC at ambient temperature, the toughness of SFRCC at low temperature before peak load can be represented by the prepeak flexural toughness ratio, and the greater the value, the better the toughness. The calculation expression is as follows:

$$\begin{cases} f_{e,j} = \dfrac{\Omega_j L}{bh^2 \delta_j} \\ R_{e,j} = \dfrac{f_{e,j}}{f} \end{cases}, \tag{4}$$

where $\Omega_j$ (N·mm) is the area enclosed by the load–displacement curve of SFRCC from the origin to $\delta_k$; $\delta_j$ (mm) is the displacement value corresponding to $j$-times peak load $P_u$, $f$ (MPa) is SFRCC flexural strength; $L$ (mm) is the span between the test beam supports; $b$ (mm) is the section width; and $h$ (mm) is the height of the section.

With $j$-values of 0.25, 0.5, 0.75, and 1, the prepeak flexure of SFRCC specimens with different fiber content is shown in Figure 9. It can be seen: before the load reaches $0.75P_u$, the prepeak flexural toughness ratio of SFRCC changes stably with the decrease of temperature. Under the same temperature condition, the prepeak flexural toughness ratio increases

by about 0.12 with an increase of $0.25P_u$. Between $0.75P_u$ and $P_u$, the prepeak flexural toughness ratio of the peak front fluctuates greatly with the decrease in temperature, and the prepeak flexural toughness ratio increases obviously at the same temperature, indicating that the steel fiber has no obvious toughening effect on the matrix before the load reaches $0.75P_u$, and the increase of matrix toughness is mainly affected by the change of temperature. After the load reaches $0.75P_u$, the synergistic effect of steel fiber and low temperature makes the prepeak flexural toughness ratio change obviously, and at the same time makes the toughness of SFRCC greatly improved.

Combined with the test results, the following methods are suggested to evaluate the flexural toughness of SFRCC at low temperatures:

$$T = \frac{E_{0.75P_u,k}L}{bh^2\left(L/k - \delta_{0.75P_u}\right)}, \tag{5}$$

where $T$ (MPa) is the flexural toughness index and $E_{0.75Pu,k}$ (N·mm) is the area surrounded by $0.75P_u$ displacement to failure displacement $L/k$ in the load–displacement curve, that is the area surrounded by CEI curve in Figure 8. The $k$ value is based on the actual failure displacement. $\delta_{0.75Pu}$ (mm) is the displacement when the load is $0.75P_u$; $L$ (mm) is the span between the test beam supports; $b$ (mm) is the section width; and $h$ (mm) is the height of the section.

The flexural toughness index, $T$ reflects the toughness property of steel fibers in SFRCC when they start to play a role in the flexural failure of the specimen. The larger $T$ is, the better the flexural toughness is. Compared with JSCE-SF4 [20] and ASTM C 1609 [21], this method avoids the difficulty of determining the initial crack point and the influence of the softening of the bearing contact point on the slope of the initial upward section of the load–displacement curve at the initial loading stage. Before the peak load, starting calculation from the rising part of the load–displacement curve where steel fiber plays a major role, the influence of the matrix toughness enhancement caused by low temperature on the toughening effect evaluation of steel fiber is reduced. After the peak load, the failure displacement $L/k$ can be calculated with different displacements, and the results can more truly reflect the low-temperature flexural toughness level of SFRCC, which meets the needs of practical engineering structure calculation.

## 5. Flexural Property and Mechanism Analysis of SFRCC at Low Temperature

*5.1. Effect of Low Temperature on Flexural Toughness of SFRCC.* The matrix energy absorption curve obtained from Equation (1) is shown in Figure 10. According to pore size, the matrix can be divided into tubular pore water, capillary pore water, and gel pore water [23]. Low temperature will change the form and distribution of water in SFRCC, and the freezing point of water in different pore sizes is different [24]. The pore water inside the matrix gradually freezes according to the pore size, resulting in volume expansion, which

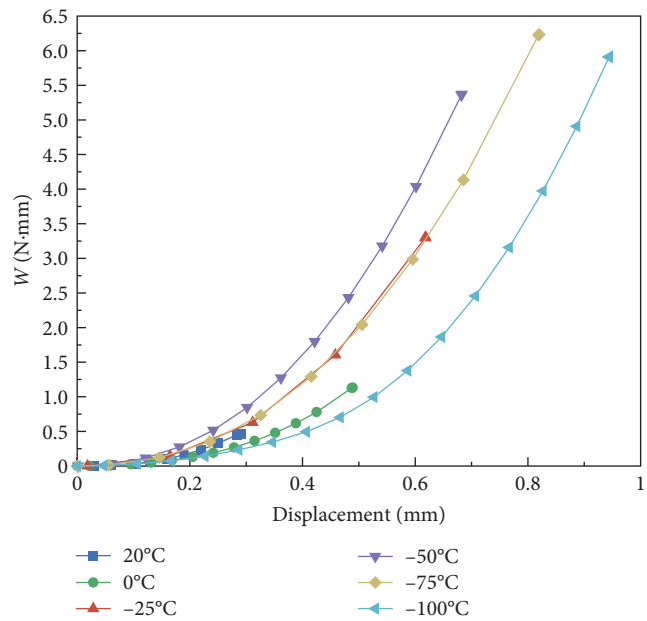


Figure 10: Energy absorption curve of matrix.

increases the compactness of the SFRCC matrix under the action of low temperature. Meanwhile, the formation of ice crystals increases the strength of the matrix and the bonding property of the matrix in the fracture transition zone, which increases the energy required for failure. It can be seen: the matrix toughness increases significantly with the decrease in temperature, which is consistent with Pigeon and Cantin [13] research conclusion.

The flexural toughness index of SFRCC obtained from Equation (5) is shown in Figure 11. It can be seen: the flexural toughness of SFRCC can significantly improve than that of ambient temperature when the temperature is lower than −25°C, as well as the flexural toughness of SFRCC increases first and then decreases with the decrease of temperature, indicating that there is a critical point for flexural toughness at low temperatures, and the critical point is around −50–−75°C. The flexural toughness of 0.5vol%, 1.0vol%, 1.5vol%, and 2.0vol% increases respectively by 138%, 217%, 354%, and 330% at low temperature. With a further decrease in temperature, the toughness of SFRCC decreases. At −100°C, the flexural toughness of 0.5vol%, 1.0vol%, 1.5vol%, and 2.0vol% increases respectively by 69%, 88%, 154%, and 236%. Kim et al. [25] came to a similar conclusion.

The reasons for the positive and negative effects of low temperatures are: matrix internal water can be divided by combined with matrix ability strong or weak chemical combined water evaporation ($\alpha$-$H_2O$) and water ($\beta$-$H_2O$), the strength of SFRCC before $\beta$-$H_2O$ fully freezing increased significantly, it leads the distortion of the energy needed and toughness to increase, meanwhile, when water is frozen during phase transition, hydrostatic pressure will be generated in a limited space, and the saturated vapor pressure of ice is lower than that of water. As the pressure in pores rises, the unfrozen water will be forced to migrate in the pores, resulting in osmotic pressure on the frozen area and gradually

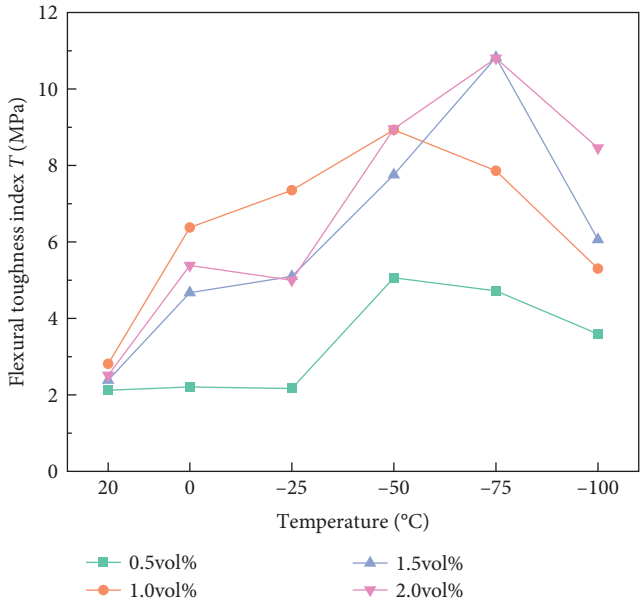


FIGURE 11: Flexural toughness index of SFRCC.

compacting the matrix. After the incorporation of steel fibers, as steel fibers are hydrophilic fibers, the hydration reaction of cement near the fibers is relatively full, and the concentration of water molecules is also relatively high [26]. The freezing of pore water enhances the strength of the matrix and the bonding ability between the matrix and steel fibers [15]. It is more difficult to pull out and slip the steel fiber, and the specimen will absorb more energy during the deformation process, which improves the flexural toughness of the SFRCC. But strength growth has slowed due to water phase change freeze after $\beta$-$H_2O$ completely frozen, and with the further decrease of temperature, the cold brittleness phenomenon is intensified, and the low-temperature effect causes the contraction of C–S–H gel chain length to shorten, resulting in the leaching of $Ca^{2+}$ inside the gel and enrichment on the surface [27, 28], which further weakens the deformation ability of SFRCC and decreases the toughness.

*5.2. Effect of Steel Fiber on Flexural Toughness of SFRCC.* Thomson [29] obtained the solid thermodynamic formula in the form of Equation (6) in the case of first-order approximation:

$$\frac{\Delta_T}{T} = -\eta \frac{\alpha}{C} \sigma, \tag{6}$$

where $\Delta_T$ is the material temperature change; $T$ is the material temperature; $\eta$ is the proportional coefficient; $\alpha$ is linear expansion coefficient; $C$ is heat capacity per unit volume; and $\sigma$ is mechanical stress. According to the principle of weighted average accumulation of heat capacity of concrete materials [30] and weighted by mass percentage, Equation (6) can be written as:

$$\frac{\Delta_T}{T} = -\eta \left( \frac{\alpha_c}{C_c} \omega_c + \frac{\alpha_{SF}}{C_{SF}} \omega_{SF} \right) \sigma, \tag{7}$$

where $\alpha_c$ and $\alpha_{SF}$ are respectively the linear expansion coefficients of the SFRCC matrix and steel fiber. $C_c$ and $C_{SF}$ are respectively the heat capacities of matrix and steel fiber. $\omega_c$ and $\omega_{SF}$ are respectively the percentages of matrix and steel fiber in the total mass of SFRCC.

Khayat and Polivka [31] and Elices et al. [32] have shown that the heat capacity and linear expansion coefficient of steel remain constant in the range of 70–−165°C, and the heat capacity of concrete decreases with the decrease of temperature when it is above 0°C and increases with the decrease of temperature when it is below 0°C, due to the liquid–solid phase mutation of water. According to Equation (6), temperature affects the heat capacity and expansion coefficient by affecting the physical state of the components of SFRCC, resulting in volume strain and stress concentration in SFRCC. The addition of steel fibers can change the thermal conductivity of the matrix, and the uniformly distributed steel fibers form a three-dimensional network structure in the matrix that promotes heat flow. It can stably transfer the internal expansion force, hydrostatic force, and permeability force caused by temperature change evenly within the specimen, inhibit the generation and development of microcracks and reduce the damage caused by frost swelling and uneven thermal conductivity of SFRCC. Figure 11 shows that increasing steel fiber content can effectively enhance low-temperature toughness. When the specific volume content of 1.0vol%, 1.5vol%, and 2.0vol% of SFRCC's low-temperature flexural toughness increases by about 108%, 85%, and 105% on average.

It can also be seen from Figure 11 that steel fiber content has positive and negative effects on the flexural toughness of SFRCC at low temperatures. At 20–−50°C, the optimal flexural toughness was 1.0vol%, the main reason is: the increase in steel fiber volume content indicates that the number of fiber bridging cracks in unit space increases, and the three-dimensional spatial support structure formed by it becomes more stable, which significantly improves the toughness and ultimate load of SFRCC. However, the increase of fiber content also causes fiber clumping, and the uneven dispersion leads to more initial defects and weak parts in the transition zone of the interface between steel fiber and matrix, which weakens the fiber-matrix effect and decreases the toughness and bearing capacity instead of increasing. After exposure to low temperatures, the matrix frost heave will make these weak parts evolve into harmful pores, resulting in the reduction of toughness. In the range of 20–−50°C, the flexural toughness of SFRCC with fiber volume content of about 1.0% is better, and in the range of −50–−100°C, the flexural toughness of SFRCC with fiber volume content of about 2.0% is better.

Due to the cold brittleness effect brought by low temperature, to ensure the safety and durability of the engineering structure at low temperatures, it is also necessary to consider

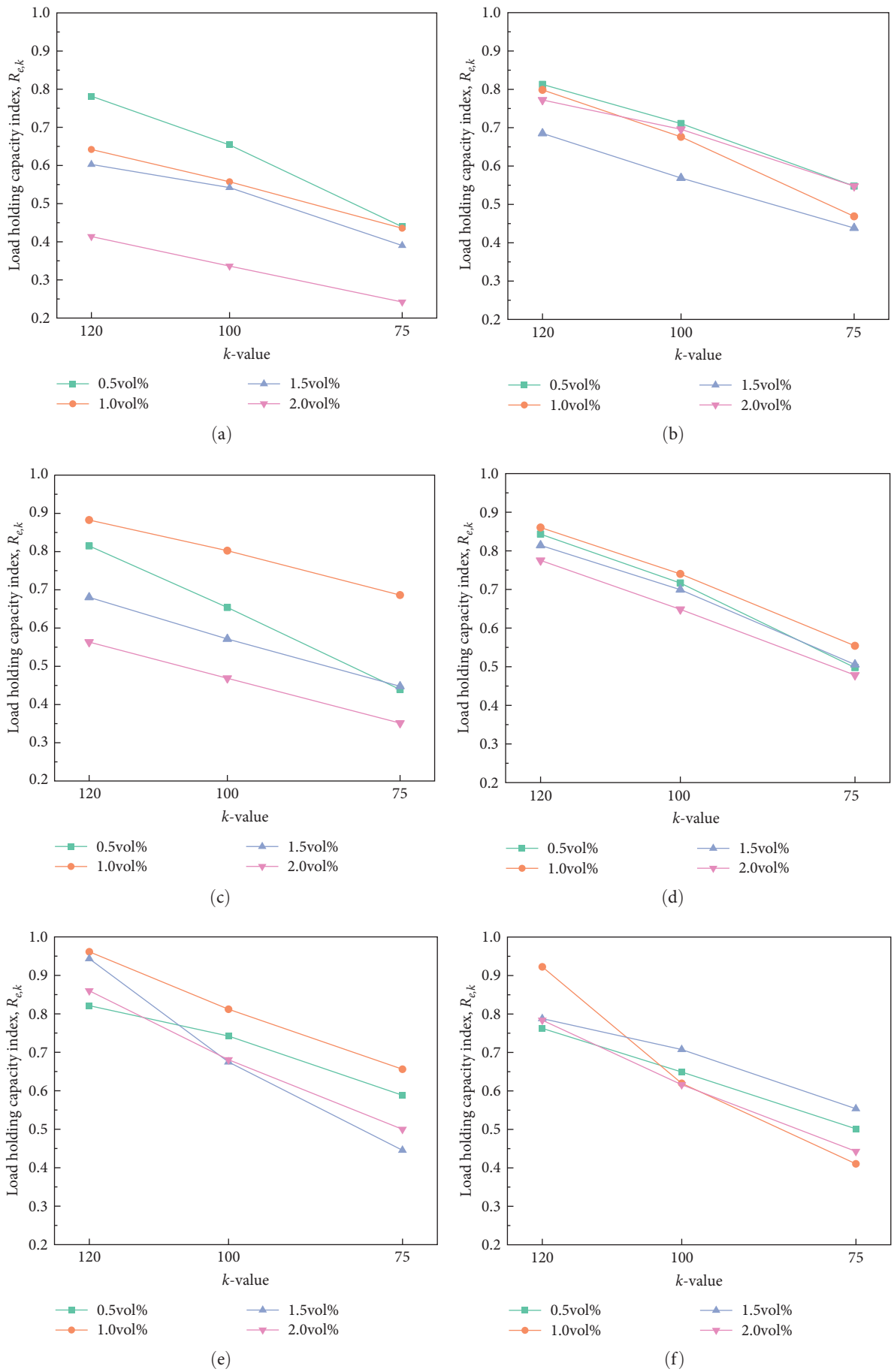


Figure 12: Load holding capacity index $R_{\varepsilon,k}$ of SFRCC: (a) 20°C, (b) 0°C, (c) −25°C, (d) −50°C, (e) −75°C, and (f) −100°C.

the load-holding capacity of SFRCC when it is continuously deformed after low-temperature action to avoid brittle failure of the engineering structure during the stress process. The load-holding capacity of SFRCC can be evaluated using the recommended methods such as Gao et al. [8], whose calculation formula is as follows:

$$\begin{cases} R_{e,k} = \dfrac{f_{e,k}}{f} \\ f_{e,k} = \dfrac{\Omega_{R,k} L}{bh^2 \delta_{R,k}} \\ \delta_{R,k} = \delta_k - \delta_P \end{cases}, \tag{8}$$

where $R_{e,k}$ is the load-holding capacity index, the larger the value, the stronger the load-holding capacity of SFRCC after the peak load. $f$ (MPa) is SFRCC flexural strength. $\Omega_{R,k}$ (N·mm) is the area enclosed by the load–displacement curve of SFRCC from $\delta_k$ to $\delta_P$. $L$ (mm) is the span between the test beam supports; $b$ (mm) is the section width; and $h$ (mm) is the height of the section. $\delta_P$ (mm) is the displacement value corresponding to peak load $P_u$, $\delta_k$ is the given calculated displacement $L/k$, and $k$ is 150,120,100, and 75 according to the engineering practice.

The load-holding capacity of SFRCC is shown in Figure 12. It can be seen that: the load-holding capacity of SFRCC decreases with the increase of deformation. The reason is that the crack propagation bypassing the steel fiber makes the steel fiber constantly pull out from the crack development, which leads to the weakening of the bridging effect and the cracking resistance and toughening effect of the steel fiber. It can also be seen that the load-holding performance of 2.0vol% is generally lower than that of 1.0vol%. The difference between them is small at 0, −50, and −100°C. When the deformation of SFRCC continues to increase to $L/75$, the load-holding performance indexes of 1.0vol% and 2.0vol% are higher than 50%. But at 20, −25, and −75°C, the load-holding capacity of 2.0vol% is significantly lower than that of 1.0vol%. At −75°C, the load-holding capacity of 2.0vol% is less than 50% when the deformation continues to increase to $L/75$, while the load-holding capacity of 1.0vol% is still about 70%. As well as 1.0vol% has a slower decay rate of load-holding capacity and can absorb more deformation work in the process of continuous deformation than 2.0vol%, indicating that 1.0vol% can better avoid low-temperature brittle fracture in the case of large deformation. This is beneficial to maintain the original stress state of the cryogenic engineering structure without brittle failure when it is subjected to sudden load.

Considering that buildings serviced in polar regions and some engineering structures in high regions are mainly in an environment not lower than −70°C [33], as well as the harm of brittle failure of engineering structures at low temperatures, combining the flexural toughness index and load-holding capacity index, the low-temperature flexural performance of 1.0vol% SFRCC is better.

## 6. Conclusions

This study conducted four-point bending tests on SFRCC beam specimens with steel fiber volume fractions ranging from 0% to 2.0% at temperatures ranging from 0 to −100°C, obtaining load–displacement curves and failure modes of the specimens. Through calculation and analysis of the load–displacement curves, the influence of low temperature and steel fibers on the flexural performance was studied, and the following conclusions:

(i) With the decrease in temperature, the ultimate load of the SFRCC matrix increases by 355% at −100°C, and the energy absorbed by the matrix increases significantly when the force is broken, and the flexural toughness is improved at the same time.

(ii) With the decrease of temperature, the ultimate load of SFRCC increases, and the slip-hardening characteristic gradually changes to slip-softening in the load–displacement curve. At the same time, the decrease in temperature leads to an initial increase and subsequent decrease in flexural toughness, and the temperature point of this transition is around −50–−75°C. However, the flexural performance at temperatures ranging from 0 to −100°C is superior to that at ambient temperature.

(iii) Low temperature and steel fiber have a coordination effect, the addition of steel fiber can significantly increase the peak load and deformation capacity, as well as improve the flexural toughness of SFRCC at 0–−100°C. However, higher steel fiber content may have detrimental effects.

(iv) The proposed method for evaluating the flexural toughness of SFRCC at low temperatures is simple and meaningful. It avoids the difficulty of determining the initial crack point and the influence of the softening of the bearing contact point at the initial loading stage on the slope of the initial upward section of the load–displacement curve and reduces the influence of the matrix toughness enhancement brought by low temperature on the evaluation of the toughening effect of steel fibers. The toughness level of SFRCC at low-temperature flexural is more truly reflected and more in line with the actual engineering structure calculation needs.

(v) Based on the flexural toughness index and load holding capacity index, the flexural toughness of SFRCC with fiber volume content of about 1.0% is better in polar cryogenic engineering.

## Data Availability

The data used to support the findings of this study are available from the corresponding author upon request.

## Conflicts of Interest

The authors declare that they have no conflicts of interest.

## Acknowledgments

This work was funded by the Natural Science Foundation of Hubei Province of China (2020CFB860).

## References

[1] K. J. Bird, R. R. Charpentier, D. L. Gautier et al., *Circum-Arctic Resource Appraisal: Estimates of Undiscovered Oil and Gas North of the Arctic Circle*, Fact Sheet, 2008.

[2] L. Zhou and S. Ding, *Forecasting Method and Application of Ice Resistance for Polar Ships*, Bilingual Press, Singapore, 2020.

[3] G. R. Harrison, "Exploratory drilling: the polar challenge," WPC 18128, 1979.

[4] G. Shan and K. Zhao, "Ultra-low temperature concrete," *Low-Temperature Building Technology*, vol. 4, no. 1, pp. 57–60, 1980.

[5] Z. Jiang and X. Li, "Experimental study on mechanical properties of mortars at an ultra-low temperature," *Journal of the Chinese Ceramic Society*, vol. 38, no. 4, pp. 602–607, 2010.

[6] X. Shi, L. Qian, and Y. Cui, "Experimental research on cryogenic temperature compressive strength of concrete under coupling action of key influencing factors," *Industrial Construction*, vol. 50, no. 1, pp. 135–141, 2020.

[7] X. Shi, Y. Cui, and L. Qian, "Experimental research on cryogenic temperature tensile strength of concrete under coupling action of key influencing factors," *Industrial Construction*, vol. 50, no. 8, pp. 85–91, 2020.

[8] D. Gao, L. Zhao, H. Feng, and S. Zhao, "Flexural toughness and its evaluation method of steel fiber reinforced concrete," *Journal of Building Materials*, vol. 17, no. 5, pp. 783–789, 2014.

[9] Y. Ye, Z. Wang, F. Xie, C. Fu, and Z. Y. Zhang, "Mechanical properties of steel fiber reinforced high-strength lightweight aggregate concrete," *Journal of Building Materials*, vol. 24, no. 1, pp. 63–70, 2021.

[10] R. Hai, P. Liu, Y. Yang, and J. Liu, "Mechanical properties of steel fiber reinforced fly ash self-compacting concrete," *Journal of Building Materials*, vol. 24, no. 1, pp. 87–92, 2021.

[11] F. S. Rostásy and K. H. Sprenger, "Strength and deformation of steel fibre reinforced concrete at very low temperature," *International Journal of Cement Composites and Lightweight Concrete*, vol. 6, no. 1, pp. 47–51, 1984.

[12] M.-J. Kim, S. Kim, S.-K. Lee, J.-H. Kim, K. Lee, and D.-Y. Yoo, "Mechanical properties of ultra-high-performance fiber-reinforced concrete at cryogenic temperatures," *Construction and Building Materials*, vol. 157, pp. 498–508, 2017.

[13] M. Pigeon and R. Cantin, "Flexural properties of steel fiber-reinforced concretes at low temperatures," *Cement and Concrete Composites*, vol. 20, no. 5, pp. 365–375, 1998.

[14] GB/T 50081-2019, "Ministry of housing and urban-rural development of the People's Republic of China," The standard for test method of mechanical properties on ordinary concrete [S]. Beijing: China Architecture & Building Press, 2019.

[15] J. Xie, H. J. Li, Z. M. Nie, and H. H. Wu, "Experimental study on bond properties between reinforcement and concrete at low temperatures," *China Civil Engineering Journal*, vol. 45, no. 10, pp. 31–40, 2012.

[16] CECS 13-2009, "China association for engineering construction standardization," Fiber-reinforced concrete test method standard[S]. Beijing: Planning Press, 2010.

[17] GB/T 50152-2012, "Ministry of housing and urban-rural development of the People's Republic of China," Concrete structure test method standard[S]. Beijing: China Architecture & Building Press, 2012.

[18] R. D. Browne and P. B. Bamfourth, "The use of concrete for cryogenic storage: a summary of research, past and present," in *Concrete Soc Cryogenic Concrete: Proceedings of the 1st International Conference*, pp. 1–135, Construction Press, London, 1982.

[19] X. Shi, C. Ma, T. Zhang, and W. Zhang, "Experimental study on compressive behavior of different strength grade concretes exposed to -190°C," *Engineering Mechanics*, vol. 34, no. 3, pp. 61–67, 2017.

[20] JCI, *JSCE-SF4 Method of Test for Flexural Strength and Flexural Toughness of Fiber Reinforced Concrete*, pp. 45–51, Japan Concrete Institute, Tokyo, 1984.

[21] ASTM. ASTM C 1609, "Standard test method for flexural performance of fiber reinforced concrete (using beam with third-point loading)," Philadelphia: ASTM Internation, 1-8, 2006.

[22] W. Xuan, W. Xu, Y. Chen, X. Chen, and X. Cheng, "Study on fracture properties of high-performance cement-based composites under different loading rates," *Materials Reports*, vol. 35, no. 22, pp. 22051–22056, 2021.

[23] R. B. Kogbara, S. R. Iyengar, Z. C. Grasley, E. A. Masad, and D. G. Zollinger, "A review of concrete properties at cryogenic temperatures: towards direct LNG containment," *Construction and Building Materials*, vol. 47, pp. 760–770, 2013.

[24] S. Xue, P. Zhang, J. Bao, L. He, Y. Hu, and S. Yang, "Comparison of mercury intrusion porosimetry and multi-scale X-ray CT on characterizing the microstructure of heat-treated cement mortar," *Materials Characterization*, vol. 160, Article ID 110085, 2020.

[25] S. Kim, D. Y. Yoo, M. J. Kim, and N. Banthia, "Self-healing capability of ultra-high-performance fiber-reinforced concrete after exposure to cryogenic temperature," *Cement and Concrete Composites*, vol. 104, Article ID 103335, 2019.

[26] N. Ranjbar, S. Talebian, M. Mehrali, C. Kuenzel, H. S. C. Metselaar, and M. Z. Jumaat, "Mechanisms of interfacial bond in steel and polypropylene fiber reinforced geopolymer composites," *Composites Science and Technology*, vol. 122, pp. 73–81, 2016.

[27] X. Zhu, C. Qian, B. He, Q. Chen, and Z. Jiang, "Experimental study on the stability of C-S-H nanostructures with varying bulk $CaO/SiO_2$ ratios under cryogenic attack," *Cement and Concrete Research*, vol. 135, Article ID 106114, 2020.

[28] X. Zhu, Z. Jiang, B. He, and Q. Chen, "Investigation on the physical stability of calcium-silicate-hydrate with varying $CaO/SiO_2$ ratios under cryogenic attack," *Construction and Building Materials*, vol. 252, Article ID 119103, 2020.

[29] W. Thomson, *Mathematical and Physical Paper*, Focal Press, London, 1990.

[30] D. Chen and C. Qian, "Research on determination and calculation method of specific heat capacity of cement-based materials," *Journal of Building Materials*, vol. 2, pp. 127–131, 2007.

[31] K. H. Khayat and M. Polivka, "Cryogenic frost resistance of lightweight concrete containing silica fume," *Trondheim Conference*, vol. 114, Article ID 915, 1989.

[32] M. Elices, H. Corres, and J. Planas, "Behavior at cryogenic temperatures of steel for concrete reinforcement," *ACI*, pp. 405–411, 1986.

[33] J. Liu, T. Jiang, Y. Yang, and Y. Zhou, "Effect of PVA fiber on dynamic and static mechanical properties of concrete under freeze-thaw cycles at extremely low temperature (-70°C)," *Journal of Wuhan University of Technology-Materials Science Edition*, vol. 38, no. 2, pp. 366–373, 2023.